bution of turbulence to high frequencies. This is in agreement with the qualitative observation of Thompson,[10] that the addition of the LEX fence results in the formation of a secondary fence vortex that interacts with the primary LEX vortex, possibly altering the frequency of any unsteady flow component downstream of the vortex breakdown. The redistribution of turbulence to higher frequencies is a desired feature of adding the LEX fences because, if done properly, it could move turbulence away from the critical low frequencies of the vertical tail. The present data corroborate those of recent wind-tunnel and flight measurements of tail buffet on the F/A-18,[1-4] which have shown that the LEX fence extends the turbulence frequency content over a wider band and reduces the fin tip acceleration considerably.

Conclusions

A low-speed wind tunnel investigation was conducted to examine the vortex wake downstream of a 3% scale model of the YF-17 at high AOAs. The hot-wire and power spectrum measurements were made in the velocity range of 10–50 m/s with and without the LEX fences. The following conclusions are drawn from this investigation:

1) The maximum turbulent fluctuation at a near downstream station just aft of the model occurred with the model oriented at 25-deg AOA.

2) The addition of LEX fences increased the spectral levels and shifted the power spectrum toward higher frequencies.

Acknowledgments

This work was undertaken in support of NASA Ames Research Center's wind tunnel investigation of a full-scale F/A-18 as part of NASA's high alpha technology program. Special thanks go to Larry Meyn, Wendy Lanser, and Jim Ross of NASA Ames Research Center.

References

[1]Lee, B., and Brown, D., "Wind Tunnel Studies of F/A-18 Tail Buffet," AIAA Paper 90-1432, June 1990.

[2]Martin, C. A., and Thompson, D. H., "Scale Model Measurements of Fin Buffet Due to Vortex Bursting on the F/A-18," HTP-5 Workshop on Vortical Flow Breakdown and Structural Interactions, NASA Langley Research Center, Hampton, VA, Aug. 1991.

[3]Lee, B. H. K., "Unsteady Pressure Measurements on the F/A-18 Vertical Tail," HTP-5 Workshop on Vortical Flow Breakdown and Structural Interactions, NASA Langley Research Center, Hampton, VA, Aug. 1991.

[4]Zgela, M., and Poirel, D., "Flight Test Investigations of Tail Buffet on the F/A-18 Aircraft," HTP-5 Workshop on Vortical Flow Breakdown and Structural Interactions, NASA Langley Research Center, Hampton, VA, Aug. 1991.

[5]Sellers, W. L., Meyers, J. F., and Hepner, T. E., "LDV Surveys over a Fighter Model at Moderate to High Angles of Attack," Society of Automotive Engineers TP 881448, Oct. 1988.

[6]Komerath, N. M., Schwartz, R. J., Percival, S., and Kim, J. M., "Unsteady Vortex Flow Measurements over Twin-Tailed Aircraft at High Angles of Attack," AIAA Paper 91-0279, Jan. 1991.

[7]Frink, W. D., Jr., "Hot-Wire Surveys in the Vortex Wake Downstream of a Three-Percent Fighter Aircraft Model at High Angles of Attack," M.S. Thesis, Naval Postgraduate School, Monterey, CA, Dec. 1990.

[8]Hebbar, S. K., Platzer, M. F., and Frink, W. D., Jr., "Vortex Wake Investigation of Twin-Tail Fighter Aircraft Model at High Angles of Attack with and Without LEX Fences," AIAA Paper 93-0868, Jan. 1993.

[9]Hebbar, S. K., and Sommers, J. D., "Wind Tunnel Studies of Support Strut Interference on a 3% YF-17 Fighter Aircraft Model at High Angles of Attack," AIAA Paper 90-3083, Aug. 1990.

[10]Thompson, D. H., "Water Tunnel Flow Visualization of Vortex Breakdown over the F/A-18," Aeronautical Research Labs., Flight Mechanics Rept. 179, Australia, Dec. 1990.

Turbulent Effects on Parachute Drag

Mayer Humi*
Worcester Polytechnic Institute,
Worcester, Massachusetts 01609

I. Introduction

ONE of the key indicators to measure the overall performance of fully deployed parachutes is the value of the drag coefficient.[1-3] Recently,[4] a wind-tunnel experiment was performed to measure the time-average value of this coefficient for a "parachute-like body" that was nonporous but "somewhat compliant." The objective of this Note is to compare this experimental result with the predictions of different turbulence models in different CFD implementations. However, no attempt will be made here to compare the local values for the pressure and velocity that were obtained in these simulations. Furthermore, we restrict our study to the steady-state (or time-average) flow around the parachute, although other studies[5] indicate notable time-variations in the value of the drag coefficient due to vortex shedding.

To gauge the importance that turbulent effects have on the value of the drag coefficients, one can use dimensional analysis. This analysis shows[6] that for laminar flow parallel to a finite flat plate the drag coefficient cd is proportional to $(Re)^{1/2}$ (where Re is the Reynolds number), on the other hand when turbulence effects are taken into account we obtain that $cd \approx (u/U)^2$, where u is the turbulent velocity residual in the wake and U is the freestream velocity. Consequently, one is led to expect that turbulent effects will have critical importance in the correct computation of this coefficient.

For parachutes, the need for this study is accentuated further by the fact that the flowfield around parachutes have three length scales. The first is the parachute span that is of the order of 10 m, the second is its thickness that is of the order of 10^{-3} m, whereas the third is related to the wake whose size can exceed 200 m. To resolve the flowfield under these conditions requires careful adjustments of the grid and the turbulence model to obtain convergence of the solution and valid results.

II. Turbulence Models and CFD Tools

To simulate incompressible fluid flow one has to solve Navier-Stokes equations, which in nondimensional form are

$$\nabla \cdot u = 0$$

$$\frac{\partial u}{\partial t} + (u \cdot \nabla)u = -\nabla p + \frac{1}{Re}\nabla^2 u$$

In these equations, u is the fluid velocity, p is the pressure, and Re is the Reynolds number, which is defined as

$$Re = (UL/\nu_0)$$

Here, U and L are the characteristic velocity and length, and ν_0 is the dynamic viscosity of the fluid. The basic modeling assumption is that ν is actually a dynamic variable whose actual value at each point depends on the local flow conditions. Thus

$$\nu = \nu_T + \nu_0$$

where ν_t is the "turbulent viscosity."

Many turbulence models for fluid flow exist in the literature.[7] Of these models the most important from an engi-

Received April 19, 1994; revision received June 29, 1994; accepted for publication Sept. 25, 1994.

*Professor of Mathematics, Mathematical Science Department, 100 Institute Road.

Table 1 CFD packages used

CFD package	Methodology	Source
FIDAP®[a]	Finite elements	FIDAP®
OVERFLOW	Finite differences	NASA Ames
NISA®[b]-fluid	Finite element	EMRC
DTNS	Finite volume	U.S. Navy

[a]Trademark of Fluid Dynamics International, Evanston, IL.
[b]Trademark of EMRC, Troy, IL.

neering point of view are the k-ε model[7] and various algebraic models such as the Baldwin-Lomax and its variants.[7] Implementations of these models exist in various CFD packages that are available commercially. Table 1 summarizes those codes that were used in this study. We observe that all of them have an implementation of the k-ε model, however, the numerical methodology varies from one code to another. For a complete description of these numerical implementations and the capabilities of these packages the reader is referred to Refs. 8 and 9.

In addition to the codes enumerated in Table 1 we used an implementation of the three-dimensional vortex algorithm (which was written by us). This algorithm employs the Smagorinski eddy-viscosity model to account for turbulence effects in the wake.[7] It might be argued that turbulence effects are already included generically in the vortex algorithm. However, due to the finite number of point vortices used in the simulation, turbulent effects could not be accounted for correctly in the large wake. Accordingly, an appropriate turbulence model has to be implemented in this region. For a full description of this algorithm we refer the reader to Ref. 10. Based on appropriate modifications of this code we can conclude that the elastic-compliant nature of the boundary (for small deformations) yields a reduction of up to 8% in the value of the drag as compared to rigid (no-slip) boundary.[11]

III. Model

To generate the basic circular parachute geometry we used two superimposed half ellipses at the origin

$$(x^2/a^2) + (y^2/b^2) = 1, \qquad x, y \geq 0$$

with $a = 3.36$, $b = 3$, which were separated by a thickness of ≈ 0.1. On the points of these curves we performed the transformation

$$\bar{x} = x \cos \Theta + y \sin \Theta + 7.25$$

$$\bar{y} = -x \sin \Theta + y \cos \Theta + 3.75$$

(with $\tan \Theta = 1.1$), which was followed by a contraction

$$\bar{\bar{x}} = \bar{x}/3, \qquad \bar{\bar{y}} = \bar{y}/3$$

In the simulations the geometry was always assumed to be axisymmetric. The computational region was $[-3, 25] \times [0, 12]$ with free-flow boundary conditions on three edges and axisymmetric constraints along $y = 0$. This region was divided into zones and in each zone an algebraic grid was generated. For simulations with finite element codes 10,000 elements (approximately) were used. On the other hand, for finite difference schemes the grid contained about 50,000 points. In all simulations we assumed that convergence was achieved when the relative errors in the pressure and velocity were less than 10^{-3}.

IV. Results

The main objective of this research was to compute the value of the drag for the given geometry using different turbulence models. However, we examined also the effects that various factors have on the aerodynamic performance of fully deployed parachutes.

A. Effect of Reynolds Number

The results for the value of the drag that were obtained seem to confirm the almost constant value of the drag for high Reynolds numbers ($Re > 10^5$). In fact, the topological structure of the computed flow around the parachute underwent little change above $Re \approx 5 \times 10^5$. The values of the drag obtained from various CFD packages (with and without the use of a turbulence model) are summarized in Table 2. We observe that, in general, the inclusion of a turbulence model tended to increase the value of the drag by 5–10%, as compared to a straightforward simulation of Navier–Stokes equations (NSE). Comparing this with the results of a wind-tunnel experiment we find that the experimental value for the drag tends to be lower than the one expected using a turbulence model. This can be explained partially by the fact that in the experiment a body with (somewhat) compliant boundaries was used and this tends to lower the drag. At least for simulations using the vortex method we can estimate[10] that this factor lowers the drag by 7–8%. Thus, the corrected value of the drag using this method should be 1.09.

B. Compressibility Effects

The OVERFLOW code uses the compressible NSE and this allowed us to investigate compressibility effects on the drag by varying the freestream Mach number. The results as shown in Fig. 1 bear on the strong dependence of the drag

Table 2 Drag coefficient at $Re \approx 10^6$

CFD Code	Turbulence model	C_D
Overflow	Baldwin-Lomax	1.08
	Baldwin-Barth	1.12
	k-ε	1.15
NISA[a]-fluid	Laminar	0.91
	k-ε	1.13
FIDAP[a]	Laminar	0.90
	k-ε	0.99
Vortex method	Smagorinski	1.18
	Laminar	0.93
DTNS	B-L	1.06
	k-ε	1.12
Experiment		1.05
Compliant boundaries		±0.05

[a]See Table 1 footnotes.

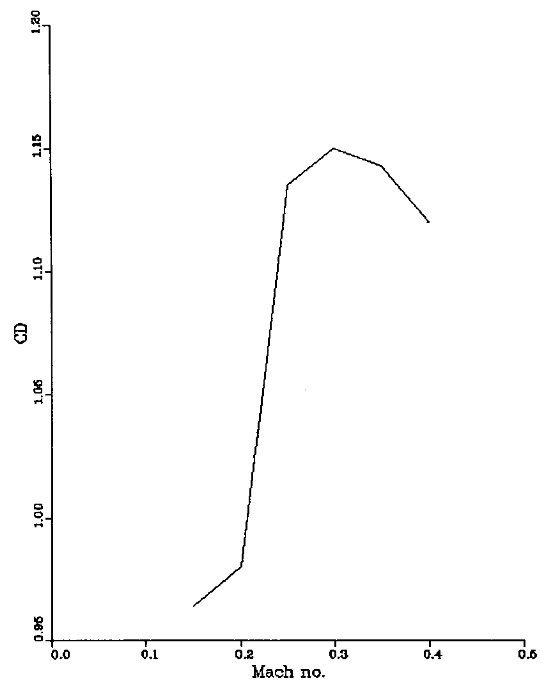

Fig. 1 C_D vs Mach number.

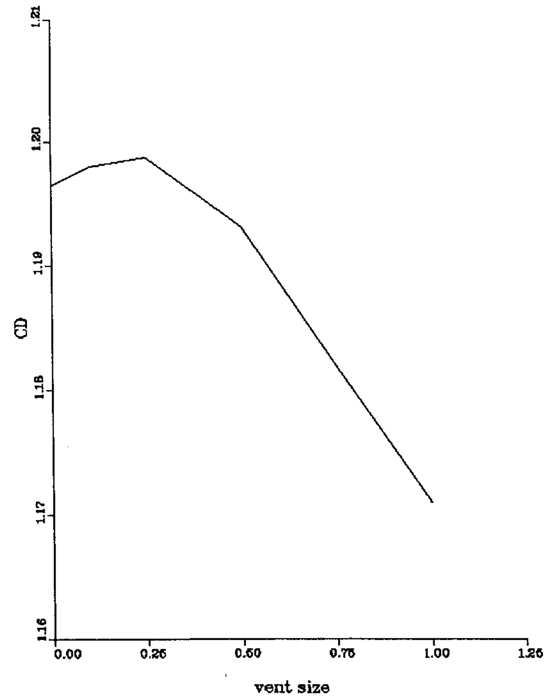

Fig. 2 C_D vs vent size, $Re = 10^6$.

on this factor. The steep dependence of the drag on the Mach number M_0 beyond $M_0 = 0.15$ is an indication of the compression wave that is being created and is consistent with experimental evidence obtained in other geometries. The small drop in the value of the drag near $M_0 = 0.4$ might be the result of numerical instabilities due to the mesh size.

C. Effect of Vent Size

Using the OVERFLOW code we simulated NSE for the geometry described in Sec. III with different vent sizes. As expected, the drag did increase as the vent size decreased. The dependence of the drag on the radius of the vent size is shown in Fig. 2. In this figure we normalized the vent size by the one used in Sec. III.

From this figure we see that for small vent sizes the drag increases considerably. This is explained by the strong vortex that is being created at the vent in this geometry.

V. Conclusions

In this research we simulated for the most part (except for the vortex algorithm) the time-independent NSE and were able to obtain time-averaged values for the drag. The results show that turbulence effects increase parachute drag by 12–15%, while canopy compliance reduces it by 7–8%. Furthermore, there is a sharp increase in the drag coefficient above Mach 0.2. We also observe that both Baldwin-Barth and the k-ε models capture correctly the effect of turbulence on the drag coefficient. The results obtained are in agreement with the experimental value when the compliant nature of the body used in the experiment is taken into account. However, based on physical arguments and results obtained using the vortex method we are led to believe that dynamical time-dependent effects can make crucial contributions to our understanding of parachute performance and design.

Acknowledgments

The author is deeply indebted to E. C. Steeves and other members of the U.S. Army RD&E Center in Natick, Massachusetts, for many discussions related to this Note. Part of this research was conducted at the center mentioned above.

References

[1]Dennis, D. R., "Recent Advances in Parachute Technology," *Aeronautical Journal*, Nov. 1983, pp. 333–342.

[2]Cockrell, D. J., "The Aerodynamics of Parachutes," AGARDOGRAPH 295, 1987.

[3]Steeves, E. C., "Analysis of Decelerators in Motion Using Computational Fluid Dynamics," *Proceedings of the AIAA 10th Aerodynamics Decelerator System Technology Conference* (Cocoa Beach, FL), 1989, pp. 269–278 (AIAA Paper 89-0931).

[4]Stein, K., private communication, U.S. Army Natick Research, Development, and Engineering Center, Natick, MA, 1991.

[5]Humi, M., "Drag Computation by Vortex Methods," *Journal of Aircraft*, Vol. 29, No. 5, 1992, pp. 819–822.

[6]Tennekes, H., and Lumley, J. L., "A First Course in Turbulence," Massachusetts Inst. of Technology Press, Cambridge, MA, 1972.

[7]Markatos, N. C., "The Mathematical Modelling of Turbulent Flows," *Applied Mathematical Modeling*, Vol. 10, No. 6, 1986, pp. 190–220.

[8]Buning, P. B., Chan, W. M., Renzi, K. J., Sondak, D. L., Chiu, I. T., and Slotnick, J. P., "OVERFLOW Users Manual," NASA Ames Research Center, Version 1.6w, Moffett Field, CA, Oct. 1992.

[9]Gorski, J. J., and Haussling, H. J., *DTNS Users Manual*, David Taylor Naval Ship RD&E Center, Bethesda, MD, 1993.

[10]Humi, M., "Three Dimensional Vortex Method for Parachutes," *International Journal for Numerical Methods in Fluids*, Vol. 16, No. 10, 1993, pp. 879–890.

[11]Benjamin, T. B., "Fluid Flow with Flexible Boundaries," *Proceedings of the 11th International Congress in Applied Mathematics* (Munich, Germany), 1964, pp. 109–126.

Estimation of Supersonic Leading-Edge Thrust by a Euler Flow Model

C. de Nicola,* R. Tognaccini,† and P. Visingardi‡
University of Naples, 80125 Naples, Italy
and
L. Paparone§
Centro Italiano Ricerche Aerospaziali, 81043 Capua, Italy

Nomenclature

AR = aspect ratio
C_A = axial force coefficient
C_D = drag coefficient
C_L = lift coefficient
$C_{L\,des}$ = design lift coefficient
C_N = normal force coefficient
M_∞ = freestream Mach number
S_s = suction parameter
α = incidence
ΔC_D = drag coefficient due to lift

Presented as Paper 94-1821 at the AIAA 12th Applied Aerodynamics Conference, Colorado Springs, CO, June 20–23, 1994; received July 28, 1994; revision received Oct. 19, 1994; accepted for publication Oct. 19, 1994.

*Associate Professor, Dipartimento di Progettazione Aeronautica, P.le Tecchio 80. Associate Member AIAA.

†Staff Research Scientist, Dipartimento di Progettazione Aeronautica, P.le Tecchio 80. Member AIAA.

‡Contract Research Scientist, P.le Tecchio 80.

§Staff Research Scientist, via Maiorise. Member AIAA.